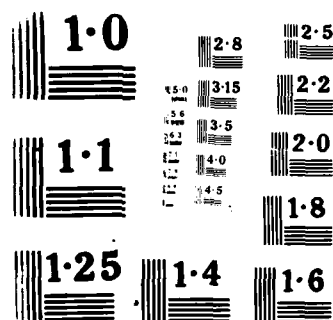


UNDERWATER EXPLOSION MODELING OF AN ENERGY ABSORPTION 1/1  
SYSTEM(U) DAVID W TAYLOR NAVAL SHIP RESEARCH AND  
DEVELOPMENT CENTER BETHESDA MD D D MORAN ET AL MAY 86  
DTNSRDC-86/012 F/G 19/4 NL

DTNSRDC-86/012

F/G 19/4

NL



NATIONAL BUREAU OF STANDARDS  
WASHINGTON, D.C. 20540

AD-A168 880

DTNSRDC-86/012

UNDERWATER EXPLOSION MODELING OF AN ENERGY ABSORPTION SYSTEM

**DAVID W. TAYLOR NAVAL SHIP  
RESEARCH AND DEVELOPMENT CENTER**

Bethesda, Maryland 20884-6000



**UNDERWATER EXPLOSION MODELING OF  
AN ENERGY ABSORPTION SYSTEM**

by

**D.D. Moran  
M.J. Dipper**

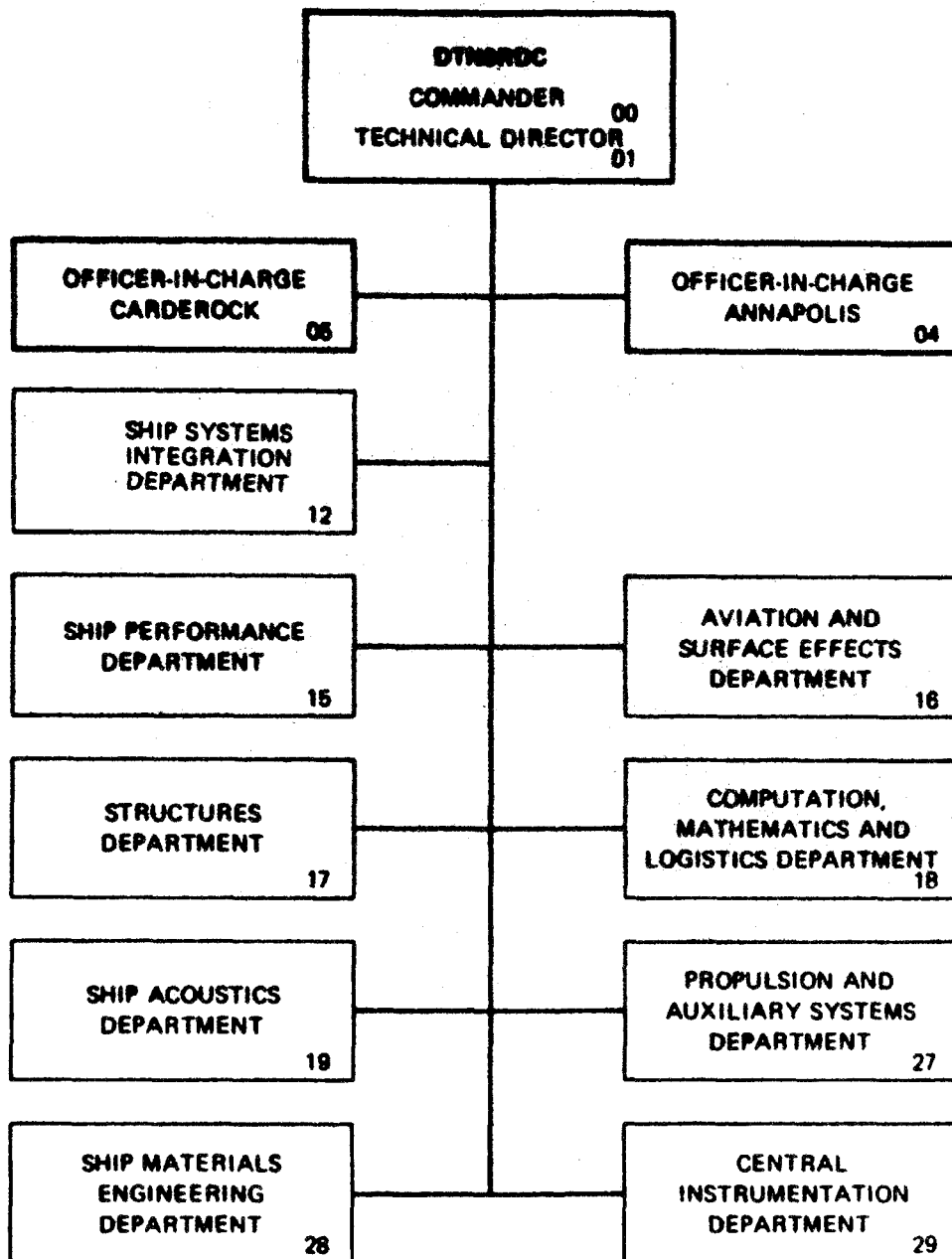
**APPROVED FOR PUBLIC RELEASE; DISTRIBUTION IS UNLIMITED.**

**SHIP PERFORMANCE DEPARTMENT  
RESEARCH AND DEVELOPMENT REPORT**

May 1986

DTNSRDC-86/012

## MAJOR DTNRDC ORGANIZATIONAL COMPONENTS



**"DESTRUCTION NOTICE** - For classified documents, follow the procedures in DoD 5230.22M, Industrial Security Manual, Section II-19 or DoD 5200.1-R, Information Security Program Regulation, Chapter IX. For unclassified, limited documents, destroy by any method that will prevent disclosure of contents or reconstruction of the document."

UNCLASSIFIED

SECURITY CLASSIFICATION OF THIS PAGE

## REPORT DOCUMENTATION PAGE

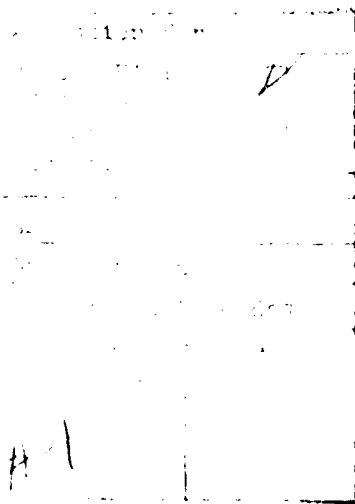
1a REPORT SECURITY CLASSIFICATION UNCLASSIFIED			1b RESTRICTIVE MARKINGS		
2a SECURITY CLASSIFICATION AUTHORITY			3 DISTRIBUTION/AVAILABILITY OF REPORT APPROVED FOR PUBLIC RELEASE; DISTRIBUTION IS UNLIMITED.		
2b DECLASSIFICATION/DOWNGRADING SCHEDULE					
4 PERFORMING ORGANIZATION REPORT NUMBER(S) DTNSRDC-86/012			5 MONITORING ORGANIZATION REPORT NUMBER(S)		
6a NAME OF PERFORMING ORGANIZATION David W. Taylor Naval Ship R&D Center		6b OFFICE SYMBOL (if applicable) Code 0120		7a NAME OF MONITORING ORGANIZATION	
6c ADDRESS (City, State, and ZIP Code) Bethesda, Maryland 20084-5000			7b ADDRESS (City, State, and ZIP Code)		
8a NAME OF FUNDING/SPONSORING ORGANIZATION Naval Sea Systems Command		8b OFFICE SYMBOL (if applicable) PMS 407		9. PROCUREMENT INSTRUMENT IDENTIFICATION NUMBER	
8c ADDRESS (City, State, and ZIP Code) National Center NC3 Alexandria, VA			10 SOURCE OF FUNDING NUMBERS		
			PROGRAM ELEMENT NO 63502N	PROJECT NO	TASK NO S0262MW001
			WORK UNIT ACCESSION NO		
11 TITLE (Include Security Classification) UNDERWATER EXPLOSION MODELING OF AN ENERGY ABSORPTION SYSTEM					
12 PERSONAL AUTHOR(S) Moran, David D. and Dipper, Martin J.					
13 TYPE OF REPORT Final		13b TIME COVERED FROM TO		14 DATE OF REPORT (Year, Month, Day) 1986, May	
15 PAGE COUNT 23					
16 SUPPLEMENTARY NOTATION					
17 COSATI CODES			18 SUBJECT TERMS (Continue on reverse if necessary and identify by block number) Explosion Modeling Pressure Chamber to Simulate Explosions		
FIELD	GROUP	SUB-GROUP			
19 ABSTRACT (Continue on reverse if necessary and identify by block number)  An investigation was conducted by the Special Ship and Ocean Systems Dynamics Branch, David W. Taylor Naval Ship Research and Development Center (DTNSRDC) to evaluate the dynamic performance of a nondetonating underwater explosion laboratory model for application in the small-scale simulation of the dynamic effects of underwater explosion pressures. The laboratory model was demonstrated with an explosion energy absorption system incorporating a flexible rubber diaphragm, filled with water, which inverts when subject to underwater explosion pressure. Explosion energy is dissipated in the work done in inverting the diaphragm and vertically accelerating the water.  A small-scale model of an energy absorption tank was constructed and tested to allow examination of operational parameters fundamental to the energy absorption concept. A technique was developed to produce a range of explosion pressures to (Continued on reverse side)					
20 DISTRIBUTION/AVAILABILITY OF ABSTRACT <input checked="" type="checkbox"/> UNCLASSIFIED UNLIMITED <input type="checkbox"/> SAME AS RPT <input type="checkbox"/> DTIC USERS				21 ABSTRACT SECURITY CLASSIFICATION UNCLASSIFIED	
22a NAME OF RESPONSIBLE INDIVIDUAL David D. Moran				22b TELEPHONE (Include Area Code) (202) 227-1275	
				22c OFFICE SYMBOL Code 0120	

UNCLASSIFIED

SECURITY CLASSIFICATION OF THIS PAGE

(Block 19 continued)

excite the energy absorption tank. The technique utilized high speed photography allowing visualization of the operational performance of a tank which has been subjected to an underwater explosion event. Flexible diaphragm inversion and water acceleration demonstrate distinct dynamic trends and are unsteady processes. The experimental results indicate that the dynamic trends characterizing these processes were repeatable in form over the range of explosion pressures. Forces obtained through this technique represent forces imparted to the tank through the resistance screens and top grate as impediments to water flow. Water flow impedance provided by a resistance screen was found to be a function of resistance element position within the tank. The magnitude and duration of the impedance forces could be changed through variation of the resistance element vertical configuration. The results of this investigation demonstrate the capabilities of this testing technique and small-scale laboratory model.



UNCLASSIFIED

SECURITY CLASSIFICATION OF THIS PAGE

## TABLE OF CONTENTS

	Page
LIST OF FIGURES.....	iii
LIST OF TABLES.....	iv
NOMENCLATURE.....	v
ABSTRACT.....	1
ADMINISTRATIVE INFORMATION.....	1
INTRODUCTION.....	1
EXPERIMENTAL METHOD.....	2
EXPERIMENTAL ANALYSIS.....	4
SCALING.....	5
EXPERIMENTAL RESULTS.....	5
CONCLUSIONS.....	8
ACKNOWLEDGMENTS.....	9

## LIST OF FIGURES

1 - Side View of Model Explosion Energy Absorption Tank and Pressure Chamber; Principal Model Components and Transducer Arrangement.....	10
2 - Sketch of Inversion Process (for 4.3 N/cm <sup>2</sup> Peak Explosive Driving Pressure) Determined Through Stop Action Photographic Analysis--Model Test Section Configured with Top Grate Only.....	11
3 - Velocity Time Histories of the Ballast Water Leading Edge for Peak Explosive Driving Pressures Ranging from (a) 2.3, (b) 2.8, (c) 4.3, (d) 5.7 N/cm <sup>2</sup> --Model Test Section Configured with Top Grate Only.....	12
4 - Average Ballast Water Leading Edge Velocity versus Peak Driving Pressure--Average Velocities Calculated from Data Obtained Through Stop Action Photographic Analysis; Model Test Section Configured with Top Grate Only.....	12

	Page
5 - Impedance Forces on Tank Test Section and Associated Explosive Driving Pressures Superimposed from Individual Explosion Events--Demonstrates Change in Water Impedance Force Associated with Change in Model Test Section Configuration.....	13
6 - Rate of Work Performed for a Full-Test Section Configuration [(1),(2),(3),(G)].....	14

#### LIST OF TABLES

1 - Dimensions of Model Components.....	15
2 - Integrated Force for Resistance Elements--Comparison of Measured and Summed Integrated Forces for Variations on Resistance Element Configuration.....	16
3 - Energy Absorbed by Resistance Element--Comparison of Measured and Summed Energy for Variations on Resistance Element Configuration.....	17

# NOMENCLATURE

D	Shock factor: $D = \sqrt{W/R}$ [pounds <sup>1/2</sup> feet <sup>-1</sup> ]
F	Force as a function of time $F(t)$
Fn	Froude number: $Fn = V/\sqrt{gL}$
G	Top grate in the numbered screen sequence (1), (2), (3), (G)
g	Gravitational acceleration
L	Characteristic length
n	Integer time step
R	Slant distance from explosion charge point to the point of interest
t	Time
V	Velocity of water surface
W	Weight of TNT (normally given in pounds) or equivalent weight of the explosion charge
w	Work performed on structure by water passage
w	Time rate of change of work
X	Vertical position of water surface
$\lambda$	Scale ratio for the subscripted variable

## ABSTRACT

An investigation was conducted by the Special Ship and Ocean Systems Dynamics Branch, David W. Taylor Naval Ship Research and Development Center (DTNSRDC) to evaluate the dynamic performance of a nondetonating underwater explosion laboratory model for application in the small-scale simulation of the dynamic effects of underwater explosion pressures. The laboratory model was demonstrated with an explosion energy absorption system incorporating a flexible rubber diaphragm, filled with water, which inverts when subjected to underwater explosion pressure. Explosion energy is dissipated in the work done in inverting the diaphragm and vertically accelerating the water.

A small-scale model of an energy absorption tank was constructed and tested to allow examination of operational parameters fundamental to the energy absorption concept. A technique was developed to produce a range of explosion pressures to excite the energy absorption tank. The technique utilized high speed photography allowing visualization of the operational performance of a tank which has been subjected to an underwater explosion event. Flexible diaphragm inversion and water acceleration demonstrate distinct dynamic trends and are unsteady processes. The experimental results indicate that the dynamic trends characterizing these processes were repeatable in form over the range of explosion pressures. Forces obtained through this technique represent forces imparted to the tank through the resistance screens and top grate as impediments to water flow. Water flow impedance provided by a resistance screen was found to be a function of resistance element position within the tank. The magnitude and duration of the impedance forces could be changed through variation of the resistance element vertical configuration. The results of this investigation demonstrate the capabilities of this testing technique and small-scale laboratory model.

## ADMINISTRATIVE INFORMATION

This investigation was performed under the authority of the Naval Sea Systems Command, PMS 407, Task Area S0262MW001, Program Element 63502N, and sponsored by the Naval Coastal Systems Center, Code 721, under David W. Taylor Naval Ship Research and Development Center, Work Unit 1562-101.

## INTRODUCTION

The performance of underwater explosion tests on vehicle concepts and systems is a major experimental undertaking and can be quite expensive for parametric analysis of new systems. Design exercises, which require an evaluation of underwater explosion response, but do not warrant a full and detailed experimental study, may be examined on a small-scale through modeling of the explosion event. Parametric studies

fall in this category when the functional relationships between variables are more important to the design development than an exact characterization of the full-scale event. In those cases where the functional relationships can be developed empirically, the absolute magnitude of the response can be established through conventional underwater explosion testing for a single value of the shock factor D

$$D = \sqrt{W/R}$$

where W is the charge weight in pounds TNT and R is the radial distance (slant standoff) in feet. The effect of other conditions may then be established through the empirical parametric functional relationships.

In the present study, the design system under investigation is an underwater explosion energy absorption tank which may be used as an underwater explosion protection system. The energy absorption system consists of a water filled tank which has at its base a flexible rubber diaphragm containing seawater, and at its top a series of resistance screens and a top metal grate. When subjected to underwater explosion pressure, the flexible rubber diaphragm in the tank inverts, accelerating the water vertically, and dissipating explosion energy in work done on the water mass. The vertical water flow within the tank is impeded by the series of resistance screens and the top metal grate. Restriction of the water flow is intended to prevent separation of the water mass from the inverted rubber diaphragm establishing a capability for diaphragm survival when subjected to repeated pulses of underwater explosion events.

The success of the explosion energy absorption system is dependent upon its ability to stretch out the effect of the explosive forces. Operational properties fundamental to the concept are the rubber diaphragm inversion process, water motion and water impedance. The effectiveness of the resistance screens and metal grate in successfully impeding ballast-water flow without imparting damaging explosive forces to the tank is an extension of the present investigation.

An explosion modeling technique has, therefore, been developed which simulates, on a model scale, the operation of an explosion resistant energy absorption system. A small-scale model tank was constructed to represent the basic fundamental operational properties of the energy absorption system. Test data were recorded and analyzed to characterize the general dynamic performance of the system, and to demonstrate the capabilities of this technique for future design applications.

#### EXPERIMENTAL METHOD

The technique developed to simulate the dynamic performance of the explosion energy absorption system used the small-scale model tank shown in Figure 1, and the model dimensions are given in Table 1. The tank was built in two sections, both with the same square platform. The top section of the module, referred to here as the test section, houses the metal grate and the interchangeable grid resistance pieces. The top grate (G) is removable and is used only at the top of the test section. Each metal screen is removable and can be placed within the test section at any of three discrete positions.

The metal screens and grate (resistance elements) are mounted within the test section perpendicular to the ballast-water flow at the positions shown in Figure 1. The lower section, referred to here as the flexible diaphragm section, houses the flexible diaphragm which forms the bottom of the water mass container. Decoupling the test section and the tank or flexible diaphragm section allows measurement of the ballast water flow impedance provided by the series of screens and the metal deck grate. One vertical face of the model ballast tank is constructed with clear plexiglass, allowing the inversion process and water flow to be photographed.

The explosion pressure which acts on the flexible rubber diaphragm is simulated by the rapid expansion of compressed air from a pressure chamber into the flexible diaphragm section of the tank. This modeling is not meant to account for the impact effects of a water plume, but rather include only the effects of a rapid rise in pressure. The pressure chamber, shown in Figure 1, consists of a vertical aluminum cylinder closed at its lower end, and capped at its upper end by a flange with an orifice equivalent in dimension to the opening at the lower end of the model ballast tank. A rupturable seal is inserted between the two flanges closing the pressure chamber orifice. This establishes a pressure impulse source. The rupturable seal consists of two sheets of cellulose acetate with an electrical wire placed between the two sheets. The pressure chamber can be pressurized with compressed air to a known static pressure which loads the seal across the orifice. When an electrical current is applied through the wire, it overheats and burns and ruptures the acetate, allowing rapid expansion of the compressed air into the sealed volume under the tank. With a static positive air pressure in the pressure chamber, rupture of the seal marks the start of the event. The compressed air expands into the flexible diaphragm section, loading the diaphragm from below and thereby driving the inversion process. The water (mass) is thrust upward through the test section, contacting the resistance elements which impede the flow.

Evaluation of the modeled event requires measurement of the parameters controlling the inversion process and impeding the upward water flow. For testing purposes, the initial static chamber pressure must be known to establish a reference pressure associated with variations in the flow of the water mass. The time-dependent pressure rise in the flexible diaphragm section must be known to describe dynamically the pressure which loads the diaphragm thereby causing diaphragm inversion. This dynamic pressure is analogous to the pressure experienced by a diaphragm due to an underwater explosion plume. The force imparted on the test section due to ballast water flow must also be known in magnitude and duration. This force represents the shear force on the walls of the test section and drag on the resistance screens. The force due to ballast-water flow is measured to determine the effectiveness of the screens and top grate in successfully impeding this flow without imparting damaging impulsive forces to the tank.

Further characterization of the modeled event was established through high speed (500 frames) photography. Slow speed and stop action playback of the filmed event allowed detailed examination of the inversion of the flexible diaphragm and water surface deformation. Displacement and velocity

ballast-water leading edge were determined using the film speed time base. The photographic time base was synchronized with a recorded analog time base which allowed comparison of filmed results with recorded force and pressure information.

Pressure and force information which characterize the modeled explosions were recorded on analog tape. Two (Kulite 0-10 psig) pressure gauges monitored pressure in both the pressure chamber and in the flexible diaphragm section. The ballast tank test section was supported by one DTNSRDC 4-in. block gauge in a cantilevered configuration to produce force information. This force output signal was generated by electrical resistance strain gauges mounted on the block gauge flexures.

A two-phase test program was established to characterize the general dynamic performance of the tank and to demonstrate the capabilities of the testing technique. Since anticipated full-scale explosion pressures are never known a priori, the first phase of the test program included a series of explosion simulations conducted at a constant test section configuration over a range of explosion pressures. The information obtained from this phase of the program indicates the flexibility available in simulating explosion pressures with this testing technique. The second phase of the test program included a series of explosion simulations conducted over a range of test-section configurations at a constant explosion pressure. This phase was designed to investigate the change in impedance force effected through variation of the vertical location of the test section resistance pieces. The test program was designed to investigate the dynamics of the tank as a function of both explosion pressure and model configuration.

#### EXPERIMENTAL ANALYSIS

Analysis of the experimental data was straightforward involving direct observation of the modeled event and observation of films and analog oscillograph output. Frame-by-frame playback of the 500 frames/film allowed determination of displacement and velocity of the ballast water leading edge. Displacement as a function of time was treated as a discrete variable using the 2-ms time base as a reference. Velocity as a function of time was determined at these discrete time steps as the difference in two plume levels divided by the time interval according to the linear difference equation:

$$V(t_n) = (X(t_n) - X(t_{n-1})) / (t_n - t_{n-1})$$

where  $X(t)$  is the height of the ballast water leading edge at a discrete time step  $t$ , and  $V(t)$  is the velocity at each discrete time step.

The water-surface contour was also observed and sketched at each frame step. Diaphragm deformation during inversion was also observed and sketched at each time step. Examination of the flexible diaphragm section pressure time history yielded pressure rate and maximum magnitude of the pressure load on the flexible diaphragm. Examination of the test-section force-time history indicated the magnitude and duration of the force imposed on the test section by the accelerated water.

The data analysis performed to determine dynamic trends in the operational properties of the tank involved examination of superimposed pressure, force and velocity time histories. Graphic analyses of pressure-time history overlays were performed to support the assumption of repeatability in explosion pulses as a function of a fixed initial chamber pressure. Force-time histories were superimposed to obtain a measure of force variation due to a configuration change for a specific explosion pulse. Ballast water velocity plots were over-laid to characterize the inversion process over a range of pressures.

#### SCALING

The important consideration in scaling is the energy of the simulated explosion. Since energy is (directly) proportional to the characteristic pressure for a given displacement, the measured pressure in the system gives a linear scale of explosion intensity. Further, since the energy is proportional to the square of the fluid velocity, conventional Froude number ( $Fn$ ) scaling can be applied to the phenomenon such that the scale ratios are given by:

$$\lambda_v^2 = \lambda_L$$

Fresh water was used for ballast water and its weight may be scaled by the cube of the geometric scale ratio. The air pressure pulse representing the explosion pressure may be scaled directly as the scale ratio. The water velocity may be scaled by the square root of the scale ratio, and drag or force on the resistance pieces and test section may be scaled by the cube of the linear scale ratio.

#### EXPERIMENTAL RESULTS

The experimental results have been prepared to aid in the assessment of the general dynamic performance of the explosion-energy absorption systems and to indicate the capabilities of the testing technique. Dynamic properties of the ballast tank include the diaphragm inversion process, upward ballast water motion, and water-flow impedance.

In the first phase of the test program, a series of explosion simulations were conducted at a constant test-section configuration over a range of explosion pressures. The tank was configured with only a top metal grate.

Photographic records reduced to display the water surface and diaphragm contour for one explosion simulation are presented in Figure 2. The velocity of the water is defined by the leading edge of the interface and is given in Figure 3. Acceleration of the ballast water leading edge is obtainable as the slope of the velocity curve. Examination of each velocity plot reveals a stabilization in acceleration following the last major curve inflection. The slope of this trailing portion of the curve is approximately  $-1 g$ . Further examination of the photographic records indicates that the flexible diaphragm is fully inverted just prior to this stabilization. The ballast-water flow at full diaphragm inversion is subject almost entirely to acceleration due to gravity alone, as supported by this observed stabilization in acceleration.

The major inflections in the velocity curves shown in Figure 3 can be associated with the change in shape of the water-surface contour. A sketch of ballast-water contour and diaphragm deformation at discrete relative time steps is presented in Figure 2b. All events that were filmed demonstrated an initial ballast water rise with a concave up surface contour followed by a transition to a convex up contour as the water mass elongated and the leading-edge velocity increased. This transition in surface contour from concave to convex is coincident with the first major inflection observed in the velocity curves of Figure 3. The second major inflection can be linked to the occurrence of full diaphragm inversion. It should be noted that these curves and inflections denote a change in ballast-water leading-edge velocity and shape, not a change in the velocity of the entire ballast-water mass. Comparison of Figures 2a and 2b shows that the ballast-water surface contour is influenced by the shape of the flexible diaphragm which primarily causes the initial concave ballast-water contour as the diaphragm is observed to be initially constricted about its perimeter rather than inverted from its center.

The effect of simulated explosion pressure is shown through a comparison of the curves plotted in Figure 3. Inflections in these velocity curves reveal that the nonuniform diaphragm inversion process shown in Figure 2 has a significant effect on water velocity. However, the curves demonstrate a consistent dynamic trend over the entire range of explosion pressures, identifying the water motion and diaphragm-inversion process as repeatable in form and independent of the magnitude of the inversion driving pressure. The consistent increase in initial slope of the velocity curve with increased explosion-pressure magnitude shows that the inversion-driving pressure controls the magnitude of the water acceleration.

The maximum interface velocity is presented as a function of pressure in Figure 4. A data point on curve 1 is obtained by averaging all the velocity points, for a given pressure, which were determined over the entire event. A data point on curve 2 is obtained by averaging only those velocity points, for a given pressure, which were determined after full diaphragm inversion was realized. Figure 4 can be used to estimate the average velocity or near maximum velocity of the ballast-water leading edge expected for a bound, but continuous, range of explosion-driving pressures. The curves shown in Figure 4 are quadratic, thereby demonstrating the expected relationship between the pressure and the square of the velocity.

In the second phase of the test program, a series of explosion simulations was conducted over a range of test-section configurations at a constant explosion pressure. The objective of this phase of the test program was to determine the forces on the tank in impeding water flow, and to identify the dynamic behavior of particular resistance screen configurations. The positions of the removable metal screens and top-grate resistance elements are labeled in Figure 1. The lowermost screen in the test is the first contacted by the accelerated ballast water and is referred to as screen position (1). Moving upward within the test section are screen positions (2) and (3), with the deck grate at the top of the test section. Twelve screen and top grate combinations were tested at one characteristic explosion pressure. The resultant test-section forces

and associated pressure traces for each particular ballast-tank configuration are given in Figure 5. Each force trace defines the force experienced by the test section at a particular configuration due to contact with the accelerated water mass.

The dynamic behavior of the ballast-water impedance process is demonstrated clearly through the graphical superposition of individual force traces shown in Figure 5. Examination of Figure 5a indicates that the force magnitude for a fixed projected area (screen area) will decrease with an increase in positioning height of the screen within the test section. This overlay also reveals that the force duration at a fixed projected area will increase with positioning height of the screen. This effect of screen positioning is also supported by the photographic results of Figure 2. As the water is accelerated through the tank, then water plume elongates and narrows. As a result, less area of the upper position screens is contacted, but the area contacted is wetted for a longer time.

Figure 5b demonstrates the effect of summing resistance elements. This summation series spanned four explosion simulations with an initial test section configuration of the top grate only. Each successive configuration tested in this series required the addition of another metal screen, progressing to a full configuration by adding screens from the top section down. With the addition of each screen to the lower test section positions, the initial rise in force of each trace occurs at progressively earlier times and the maximum force magnitude increases. The form of the force trace becomes sharper as screens are added. Figure 5c also demonstrates the effect of summing resistance elements. In this series of explosions, the initial configurations included only the bottom screen; successive configurations in the series were established by inserting resistance elements in positions progressing upward until a full configuration was obtained. Through this addition of resistance elements, the rise in force of each trace occurs at approximately the same time, following the same general slope. Both force magnitude and duration increase with this addition of elements, with each force trace demonstrating consistency in form. Both Figures 5b and 5c demonstrate that multiple-resistance-element configuration impedance forces are a direct function of individual-element position.

Linear superposition of individual element impedance forces to approximate the force of the equivalent multiple element configuration is qualitatively appropriate when the individual element forces are known at their respective positions in the multiple configuration. This comparison can be illustrated either through an evaluation of the total force to which the model is subjected or through a calculation of the energy absorbed by the structure. In the first case the temporal force functions are shown in Figure 5. The results of integrating under the force curves are summarized in Table 2 for single and multiple combinations of resistance elements. The first five figures shown are the calculated force integrals measured on single elements. The element (0) represents the integrated shear force on the walls of the test section, and is, therefore, included in all other measured values regardless of the model configuration. For multiple-element configurations, the measured force may be compared with the equivalent-summed quantity obtained by adding the appropriate

quantities for the individual elements. The shear force (0) must be subtracted from multiple element calculations in order to obtain the figures shown in the table. For example:

$$E(1,2) = E[E(1) - E(0)] + [E(2) - E(0)] + E(0) = F(1) + F(2) - F(0) = 4.38 + 2.60 - 0.52 = 6.46$$

The comparison of measured and superimposed effects of the resistance elements can also be demonstrated through an analysis of the work done on the fluid due to water passage through the elements. The rate at which work is done ( $\dot{W}$ ) may be computed as the product of the measured force as a function of time ( $F(t)$ ) and the measured fluid velocity  $V(t)$ . An example of the rate of work function computed for a full configuration of resistance elements (1+2+3+G) is shown in Figure 6.

The total energy absorbed by the fluid is the integral of the work function over the effective time interval. Calculations of absorbed energy have been made for individual and combinations of elements through numerical integrations of functions similar to that shown in Figure 6. The results of these calculations are summarized in Table 3, which is structurally the same as Table 2. The shear force energy (0) must be appropriately removed from the summed calculations as done similarly for Table 2. Although there is good qualitative agreement between measured and superimposed quantities by both methods, the magnitude of the apparent differences cannot be explained through the results of the present experimental procedure. One would expect differences because of a slowing down of fluid by the upstream screens. However, this effect should make "summed" greater than "measured", which is not always the case. The difference may be due to other effects which cannot be identified in the experimental data.

### CONCLUSIONS

The investigation conducted addresses an evaluation of the dynamic performance of an explosion energy-absorption system. The experimental program was designed to examine the fundamental parameters which define the performance of a single tank with a flexible diaphragm and series of resistance screen elements. The parameters investigated included simulated-explosion pressures, diaphragm inversion, water acceleration and water-flow impedance. However, this series of experiments was not designed to represent the spray dome, jet, and radial plume of an underwater explosion. The tests were conducted rather to represent the effect of the water mass passing through specified resistance elements. The following conclusions are drawn from the results of this experiment:

- The technique provides an efficient means of simulating a range of explosion pressures on a small model scale.
- Examination of the inversion process reveals that the flexible diaphragm is initially constricted about its perimeter and then rolls up along its edge rather than directly inverting from the diaphragm center.

- Dynamic trends characterizing the diaphragm inversion process and water acceleration are repeatable in form over a wide range of explosion pressures.
- The forces obtained in this investigation do not represent the total forces transmitted to the tank by an underwater explosion, but rather represent forces imparted on the tank by the accelerated ballast water through contact with the impedance screens, top grate, and viscous shear on the walls of the tank.
- Water flow impedance provided by a resistance element is a function of resistance-element vertical position within the tank.
- Magnitude and duration of the water-flow impedance forces can be changed through variation in resistance-element vertical configuration.
- Linear superposition of individual-element impedance forces to approximate the force of the multiple-element configuration is only appropriate when the individual-element forces are known at their respective positions in the multiple configurations.

#### ACKNOWLEDGMENTS

The authors wish to thank A. Jennings for his assistance in designing the model and test equipment. Thanks are also due to D. Bochinski and R. Stanko for their assistance in conducting the model experiment and analyzing experiment data, and to both Dottie McLean for her careful editorial work and to G. Waldo for his many fine and carefully thought out suggestions for future presentations and applications of this material.

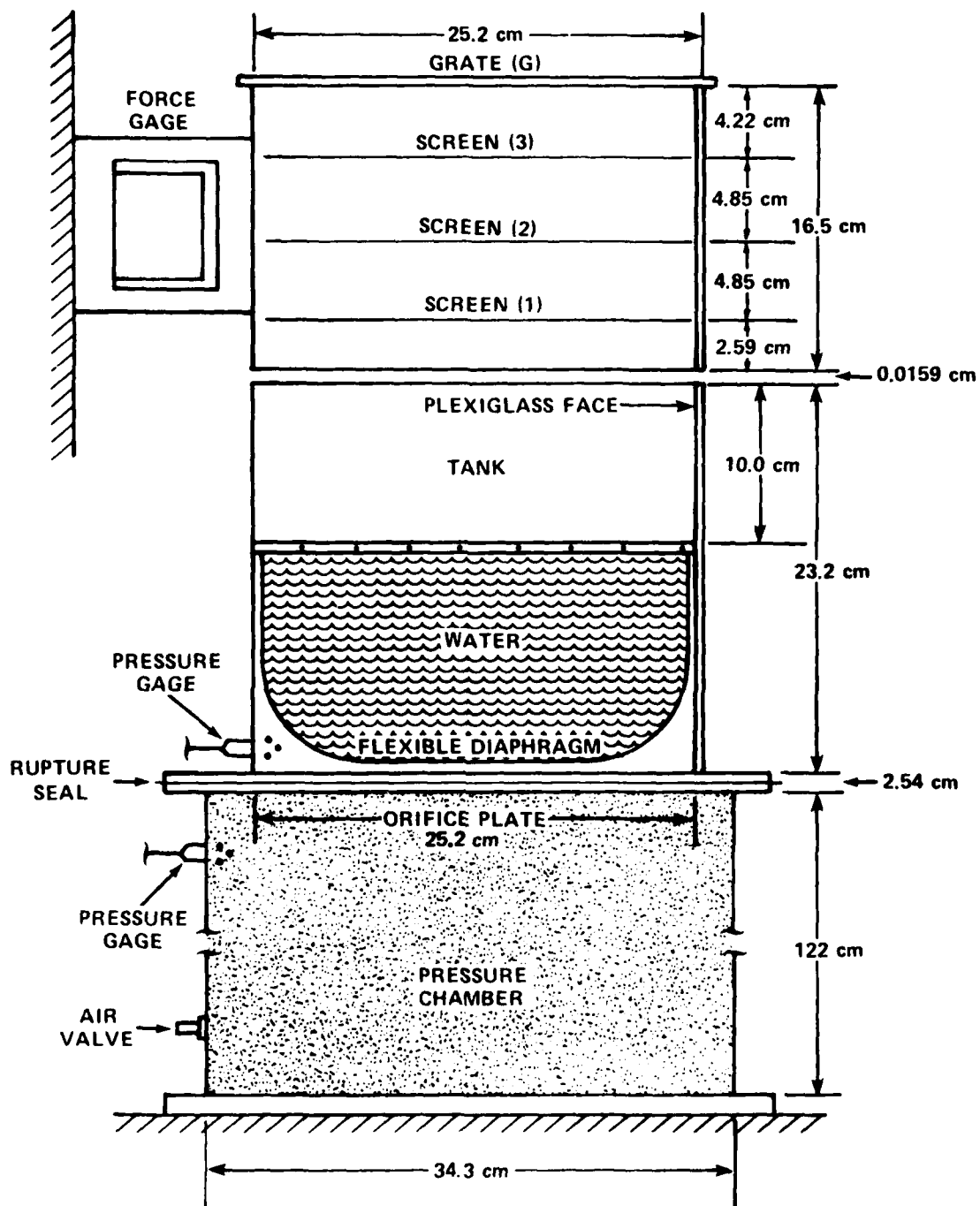


Figure 1 - Side View of Model Explosion Energy Absorption Tank and Pressure Chamber; Principal Model Components and Transducer Arrangement

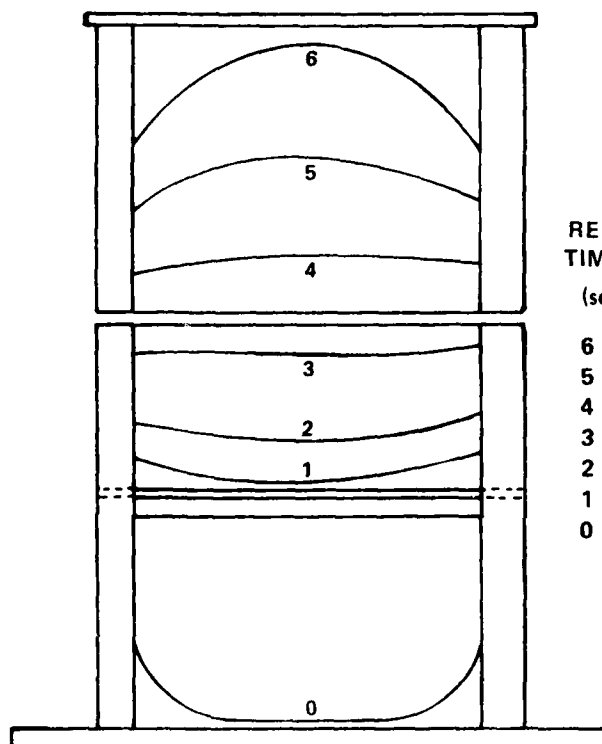


Figure 2a - Ballast Water Contour as seen Through the Plexiglass Face of the Model Energy Absorption Tank

RELATIVE  
TIME STEP  
(seconds)

6 = 0.035  
5 = 0.029  
4 = 0.023  
3 = 0.018  
2 = 0.012  
1 = 0.006  
0 = 0.000

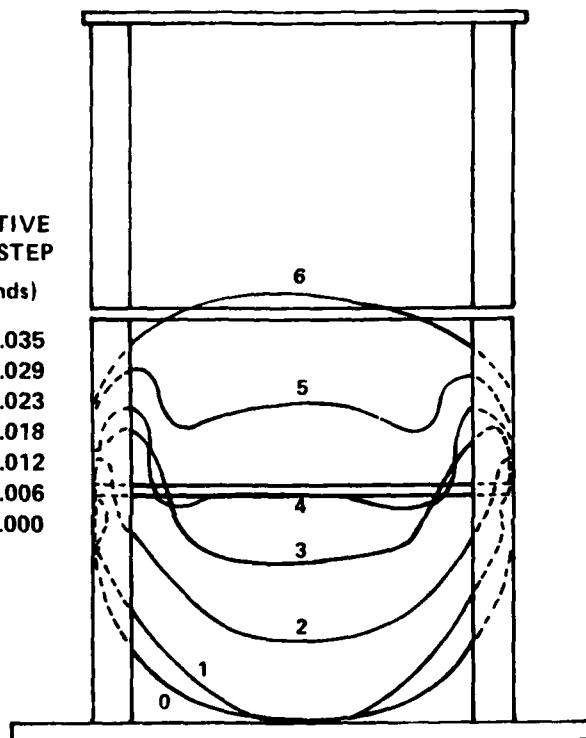


Figure 2b - Flexible Diaphragm Contour as seen Through the Plexiglass Face of the Model Energy Absorption Tank

Figure 2 - Sketch of Inversion Process (for  $4.3 \text{ N/cm}^2$  Peak Explosive Driving Pressure) Determined Through Stop Action Photographic Analysis--Model Test Section Configured with Top Grate Only

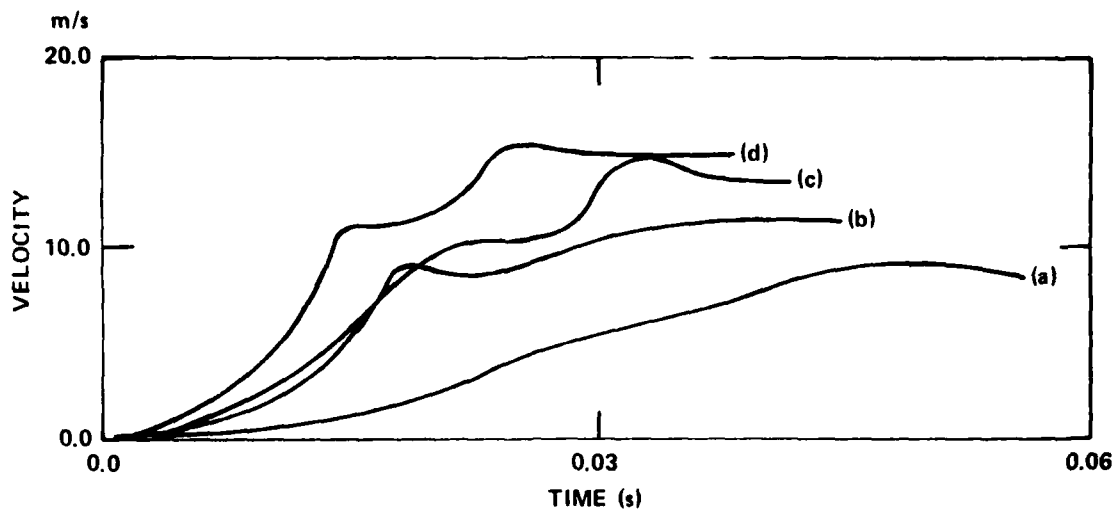


Figure 3 - Velocity Time Histories of the Ballast Water Leading Edge for Peak Explosive Driving Pressures Ranging from (a) 2.3, (b) 2.8, (c) 4.3, (d) 5.7  $\text{N/cm}^2$ -- Model Test Section Configured with Top Grate Only

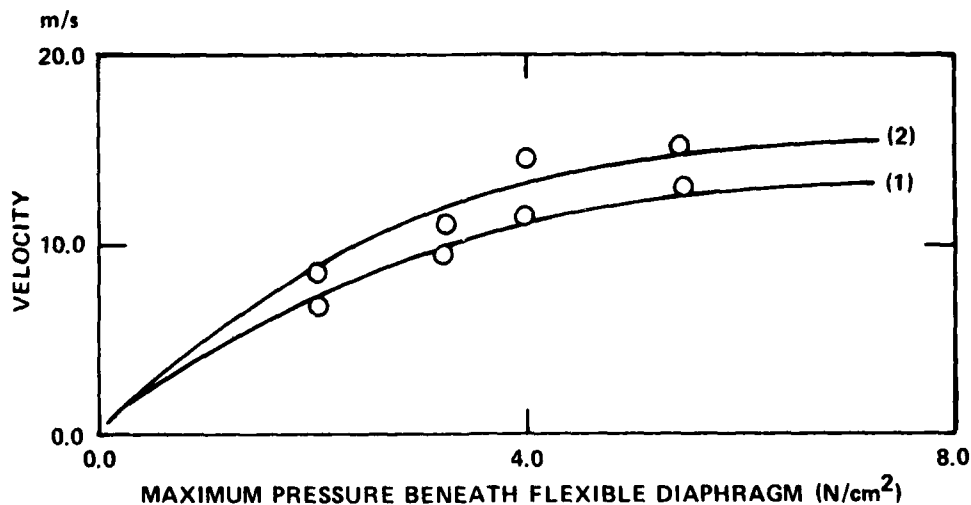


Figure 4 - Average Ballast Water Leading Edge Velocity versus Peak Driving Pressure--Average Velocities Calculated from Data Obtained Through Stop Action Photographic Analysis; Model Test Section Configured with Top Grate Only (Each Point on Curve (1) was Obtained from an Average of all Data Points Collected over an Entire Explosion Event. Each Point on Curve (2) was Obtained from an Average of Data Points Collected after Full Diaphragm Inversion was Realized.)

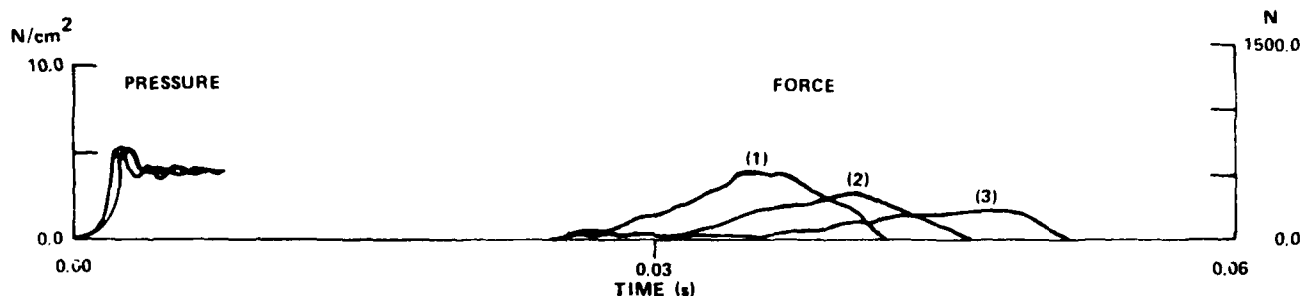


Figure 5a - One Screen Tested at Each of Three Screen Positions (1), (2) and (3)

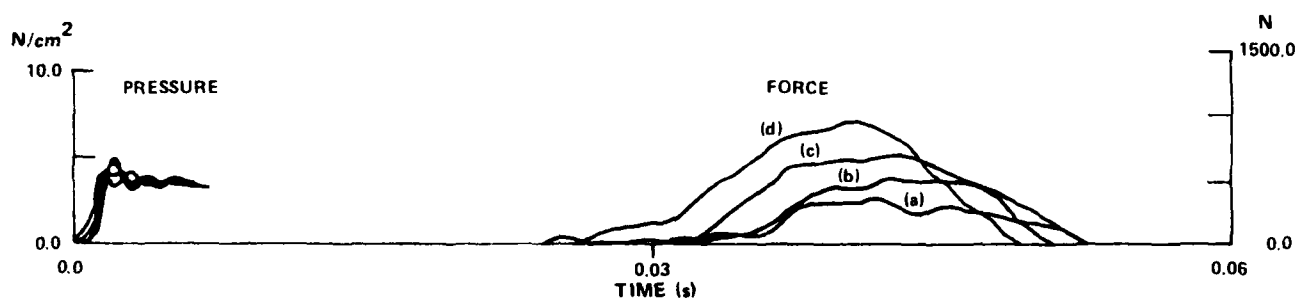


Figure 5b - An Addition of Resistance Elements to the Test Section Demonstrating the Effect of Summing Elements. Elements Added to the Test Section Beginning with the Top Grate (G), Ending in a Full Configuration (G) + (3) + (2) + (1)

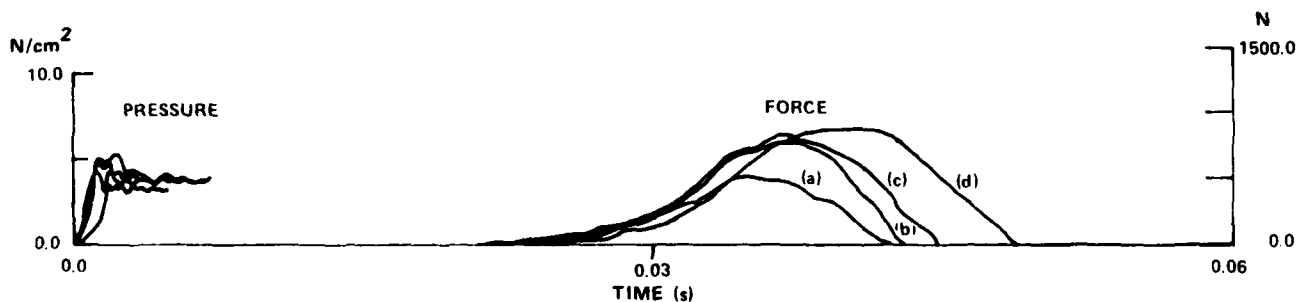


Figure 5c - An Addition of Resistance Elements to the Test Section Demonstrating the Effect of Summing Elements-- Elements Added to the Test Section Beginning with Screen (1), Ending in a Full Configuration (1) + (2) + (3) + (G)

Figure 5 - Impedance Forces on Tank Test Section and Associated Explosive Driving Pressures Superimposed from Individual Explosion Events--Demonstrates Change in Water Impedance Force Associated with Change in Model Test Section Configuration

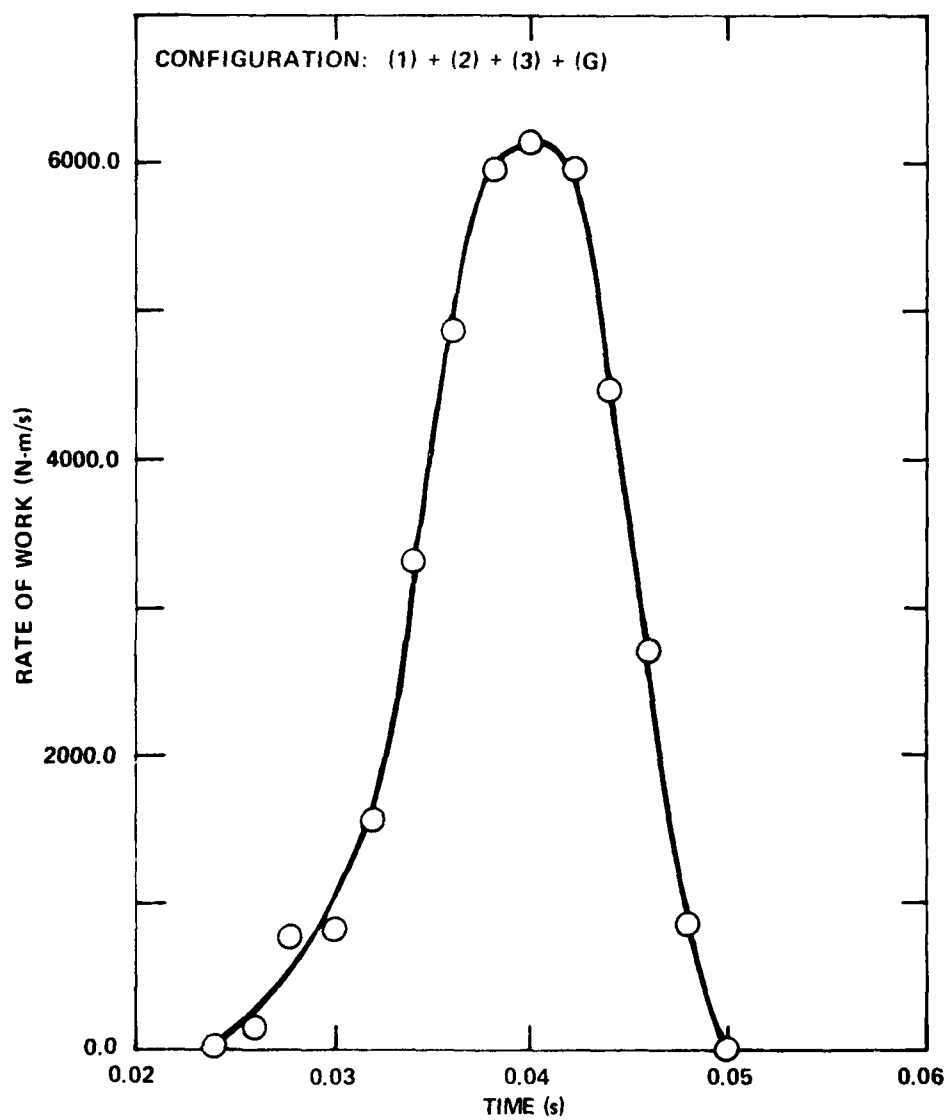


Figure 6 - Rate of Work Performed for a Full-Test  
Section Configuration [(1), (2), (3), (G)]

TABLE 1 - DIMENSIONS OF MODEL COMPONENTS

Test Section: 25.2 cm x 25.2 cm x 16.5 cm of 0.476 cm thick aluminum with a 19.1 cm x 16.5 cm x 1.3 cm clear plexiglass face

Flexible Diaphragm Section: 25.2 cm x 25.2 cm x 23.2 cm of 0.476 cm thick aluminum with a 19.1 cm x 23.2 cm x 1.3 cm clear plexiglass face

Pressure Chamber: 34.3 cm I.D. x 122.0 cm deep of 1.3 cm aluminum with 1.3 cm thick aluminum flanges capping the cylinder ends

Deck Grate: 25.7 cm x 25.7 cm x 0.64 cm brass frame with unidirectional grating strips 0.0826 cm x 0.51 cm spaced at 0.448 cm on center

Metal Screens: 0.157 cm diameter stainless steel wire woven in a square grid pattern with 1.3 cm openings: 25.1 cm x 25.1 cm overall

Flexible Diaphragm: Rubber coated nylon 5-oz sail cloth rated at 150 psi hydrostatic pressure

Rupture Seal: Cellulose acetate sheet 45.7 cm x 50.8 cm x 0.0191 cm

Rupture Wire: 16 AWG-tinned copper (wire)

Water Mass: Fresh water weight 10.7 lb (4,853 gm)

TABLE 2 - INTEGRATED FORCE FOR RESISTANCE ELEMENTS--COMPARISON OF  
MEASURED AND SUMMED INTEGRATED FORCES FOR VARIATIONS ON  
RESISTANCE ELEMENT CONFIGURATION

Resistance Elements in Model Configuration	Integrated Force, F (N - s)	
	Measured	Summed
(0)	0.52	--
(G)	4.06	--
(3)	2.29	--
(2)	2.60	--
(1)	4.38	--
(1) (2)	7.50	6.46
(1) (2) (3)	8.33	8.23
(1) (2) (3) (G)	10.83	11.77
(3) (G)	6.67	5.83
(2) (3) (G)	8.02	7.91
(1) (2) (3) (G)	11.04	11.77
(2) (3)	5.73	4.37

TABLE 3 - ENERGY ABSORBED BY RESISTANCE ELEMENT--COMPARISON OF  
MEASURED AND SUMMED ENERGY FOR VARIATIONS ON RESISTANCE  
ELEMENT CONFIGURATION

Resistance Elements in Model Configuration	Energy (N - m)	
	Measured	Summed
(0)	5.81	--
(G)	45.33	--
(3)	25.57	--
(2)	29.03	--
(1)	48.90	--
(1) (2)	83.73	72.17
(1) (2) (3)	93.00	91.89
(1) (2) (3) (G)	120.91	131.41
(3) (G)	74.47	65.09
(2) (3) (G)	89.54	88.31
(1) (2) (3) (G)	123.26	131.41
(2) (3)	63.97	48.79

# INITIAL DISTRIBUTION

## Copies

5 NAVSEA  
 1 PMS 300  
 1 PMS 303  
 1 PMS 310  
 2 PMS 407 MCM

2 NCSC  
 2 314

12 DTIC

## CENTER DISTRIBUTION

Copies	Code	Name
--------	------	------

1	012	
---	-----	--

10	012.3	
----	-------	--

1	1231	
---	------	--

1	1232	
---	------	--

1	156	
---	-----	--

20	1562	
----	------	--

1	1740.2	
---	--------	--

1	1750.2	
---	--------	--

1	177	
---	-----	--

10	5211.1	Reports Distribution
----	--------	----------------------

1	522.1	TIC (C)
---	-------	---------

1	522.2	TIC (A)
---	-------	---------

#### **DTNSRDC ISSUES THREE TYPES OF REPORTS**

- 1. DTNSRDC REPORTS, A FORMAL SERIES, CONTAIN INFORMATION OF PERMANENT TECHNICAL VALUE. THEY CARRY A CONSECUTIVE NUMERICAL IDENTIFICATION REGARDLESS OF THEIR CLASSIFICATION OR THE ORIGINATING DEPARTMENT.**
- 2. DEPARTMENTAL REPORTS, A SEMIFORMAL SERIES, CONTAIN INFORMATION OF A PRELIMINARY, TEMPORARY, OR PROPRIETARY NATURE OR OF LIMITED INTEREST OR SIGNIFICANCE. THEY CARRY A DEPARTMENTAL ALPHANUMERICAL IDENTIFICATION.**
- 3. TECHNICAL MEMORANDA, AN INFORMAL SERIES, CONTAIN TECHNICAL DOCUMENTATION OF LIMITED USE AND INTEREST. THEY ARE PRIMARILY WORKING PAPERS INTENDED FOR INTERNAL USE. THEY CARRY AN IDENTIFYING NUMBER WHICH INDICATES THEIR TYPE AND THE NUMERICAL CODE OF THE ORIGINATING DEPARTMENT. ANY DISTRIBUTION OUTSIDE DTNSRDC MUST BE APPROVED BY THE HEAD OF THE ORIGINATING DEPARTMENT ON A CASE-BY-CASE BASIS.**

END

DTIC

8-86